JOURNAL OF MATERIALS SCIENCE 31 (1996) 5513–5519

Compacting characteristics of aluminium–fly ash powder mixtures

R. Q. GUO, P. K. ROHATGI*
*Department of Materials Engineering, and *Centre for Composites, Materials Department, University of Wisconsin–Milwaukee, P. O. Box 784, Milwaukee, WI 53201, USA*

D. NATH
Department of Metallurgical Engineering Institute of Technology, Banaras Hindu University, Varanasi, 221005, India

Aluminium–fly ash powder mixtures containing 5–20 wt% fly ash were prepared using both precipitator (solid) and cenosphere (hollow) fly ash particles. These were compacted at pressures ranging from 138–414 MPa. Spring back, densification parameter, green density, green hardness and green strength of the compacts were determined as a function of compacting pressure and weight per cent of fly ash. It was observed that the spring back, green density and green strength of the compacts increased with increasing compacting pressure. Green density, green strength and green hardness of the compacts decreased, and the spring back increased, with increasing weight per cent of fly ash particles, the cenosphere particles leading to a higher spring back as compared to solid precipitator particles. At compacting pressures of the order of 345 MPa, the solid fly ash particles generally remained intact, and well distributed in the matrix, but the hollow cenosphere particles collapsed, and outer shells were present in the matrix in layered forms.

1. Introduction

Fly ash is a waste by-product of coal-based power generation plants. Millions of tons of fly ash powder are generated and a major portion of this is used in construction and land filling. Solid fly ash particles are generally collected in precipitators and have a density close to 2.1 $g\,cm^{-3}$ and hollow fly ash particles, referred to as cenospheres, are collected on the surfaces of ash ponds. The bulk of this powder is unused and landfilled, presenting disposal problems. Attempts are being made, throughout the world, to make use of this by-product for various applications. Work is in progress to explore the use of fly ash particles as a filler or reinforcements in metal as well as polymer matrices to produce useful composites. Fly ash as a filler in aluminium casting reduces cost, decreases density and increases hardness, abrasion resistance and stiffness [1–4]. Dispersion of particulate material in metal matrices results in composites with improved damping, machinability, wear and seizure resistance and low coefficients of friction and thermal expansion [5–7]. These properties are desirable in materials for automotive applications. Various components, including pistons, engine covers, connecting rods, and other castings, have been made out of aluminium alloy–fly ash composites. Under certain conditions, such composite castings are likely to exhibit segregation and non-uniform distribution of particles because of the differences in density between the fly ash particles and the melts, and poor wettability between the particles and the molten matrix alloy. The powder metallurgy technique is capable of producing certain components with a uniform distribution of particles in metal matrix composites; in fact, casting and powder metallurgy have emerged as predominant techniques for producing metal ceramic composites. The successful production of components by powder metallurgy processing depends on the characteristics of both the metal and reinforcement particles, and their compacting behaviour. There is no significant information available in the literature on characteristics of fly ash particles and the compacting behaviour of mixtures of metal powders and fly ash particles; this information is important for powder processing of metal fly ash composites. This paper deals with characterization of fly ash particles, and compacting characteristics of aluminium–fly ash powder mixtures. The information on behaviour of fly ash particles and aluminium powders during compaction of composite powder mixtures and spring-back behaviour of compacts is important in making high-performance near net-shaped parts by the powder metallurgy processes.

2. Experimental procedure

The materials used in this investigation were commercially pure (99.9%) aluminium powders supplied by Aldrich Chemicals, and fly ash powders obtained from two sources: Wisconsin Electric Power Company (precipitator fly ash) and PSI Energy (cenosphere

0022–2461

fly ash). The size of the aluminium powder was less than 106 μm. The size of precipitator fly ash was less than 75 μm, and that of fly ash cenospheres ranged from 50 –150 μm. Particle size, size distribution and morphology were determined using sieve analysis, scanning electron microscopy, and optical microscopy. Bulk density and the true density of both types of fly ash powders were determined using standard ASTM procedures. Mechanical mixtures of powders of aluminium and fly ash (5–20 wt %) were prepared using a rotating drum blender after drying them in an oven at 110 °C for 1 h. Apparent densities of aluminium–fly ash powder mixtures were also evaluated. The powder blends were then compacted at pressures ranging from 138–414 MPa using a uniaxial hydraulic press. A mixture of silicon fluid and graphite powder was used as die-wall lubricant. The die and punch consisted of hardened steel cylinders of 25.4 mm diameter. The compacts were 6.4 mm thick and 25.4 mm diameter. The green properties (density, hardness, strength and spring back) of the compacts were determined. A Rockwell hardness tester was used in L scale for hardness measurement. The green strength was evaluated according to a modified version of the ASTM 312-82 standard in order to use 6.4 mm thick cylindrical specimens. Optical and scanning electron microscopy were used for microstructural observations.

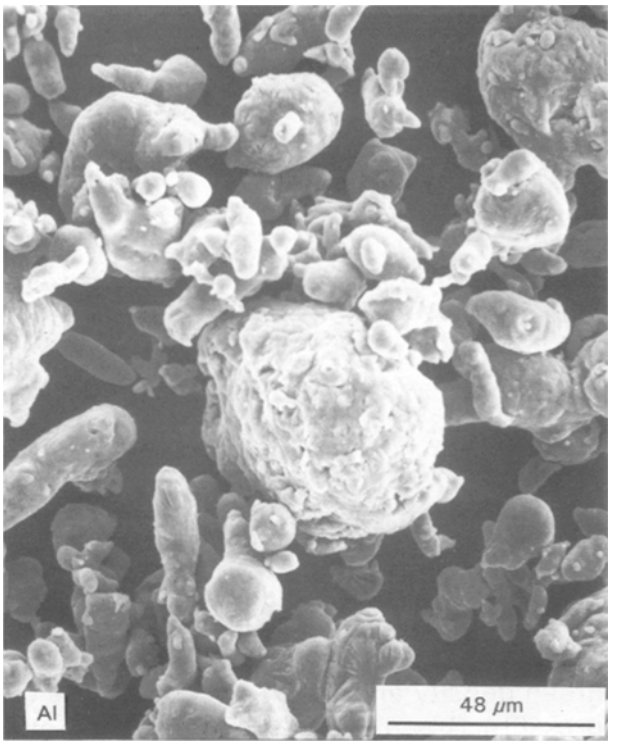

Figure 1 Scanning electron micrograph of aluminium powder.

3. Results and discussion

3.1. Powder characteristics

Characterization of powders for their shape, size, and size distribution is important for the synthesis of metal matrix composites because it determines the final porosity and strength properties of the composites. A scanning electron micrograph of aluminium powder representing its size and shape is shown in Fig. 1. This figure shows the typical appearance of both rounded and elongated shapes of atomized aluminium powder with sizes as small as 5 μm, and ranging up to as large as 50 μm.

Fig. 2 shows a scanning electron micrograph of precipitator fly ash. This figure shows that a large number of particles are spherical with their size ranging from 1–2 μm to 20 μm; the precipitator fly ash does have angular particles and has a higher density. Fig. 3 shows a photomicrograph of cenosphere fly ash particles which are predominantly spherical in shape. Typically, the wall thickness of cenospheres is in the range 4–9 μm and the ratio of wall thickness, t, to the diameter, d, of cenospheres is in the range 0.04–0.06. In addition, the walls of cenospheres have spherical porosity.

The size distribution of the as-received fly ash (both precipitator and cenosphere) determined by sieve analysis is shown in Figs 4 and 5, respectively. Fig. 4 indicates that more than 90 wt % precipitator fly ash is between 53 and 150 μm with a median size of about 70 μm. The size of cenosphere fly ash ranges from 75–150 μm with a median size of 115 μm (Fig. 5). The typical chemical compositions of precipitator and cenosphere fly ash particles are given in Table I.

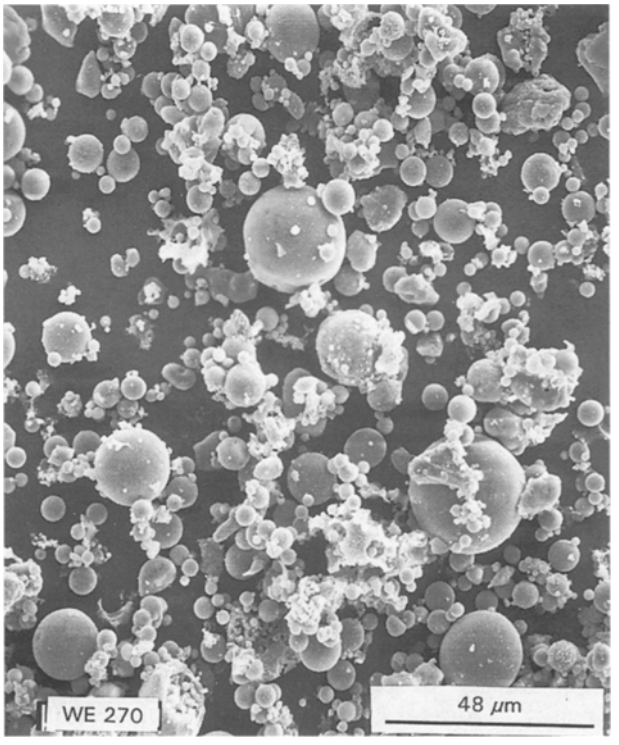

Figure 2 Scanning electron micrograph of precipitator fly ash.

The bulk density, tap density, and true density of precipitator ash of different sizes is shown in Fig. 6. It may be noted that these densities decrease with an increase in particle size, especially above a size of 75 μm; this may be due to a greater degree of porosity in larger fly ash particles.

The measured bulk density and true density of cenosphere fly ash are shown in Fig. 7. It reveals that cenosphere fly ash has very low densities

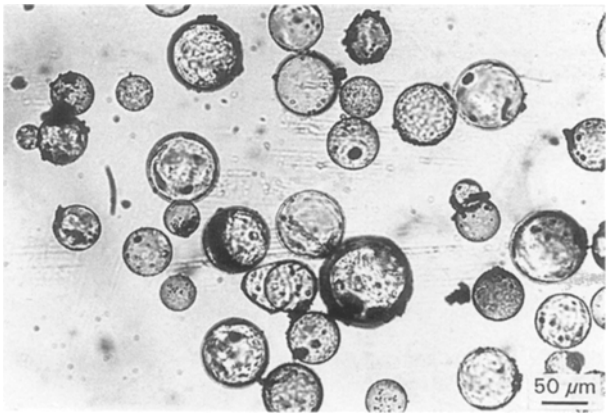

Figure 3 Photomicrograph of cenosphere fly ash.

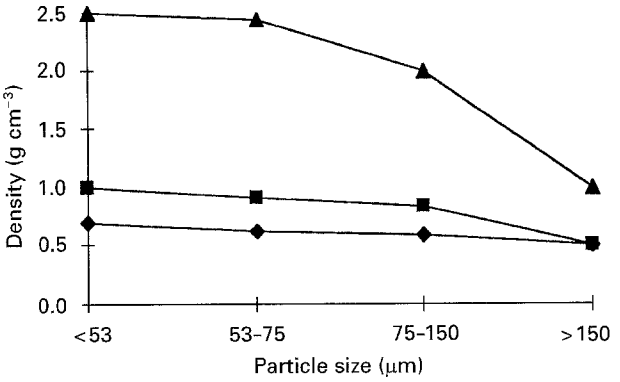

Figure 6 Apparent densities and true densities of different sized precipitator fly ash: (◆) bulk, (■) tap, (▲) true.

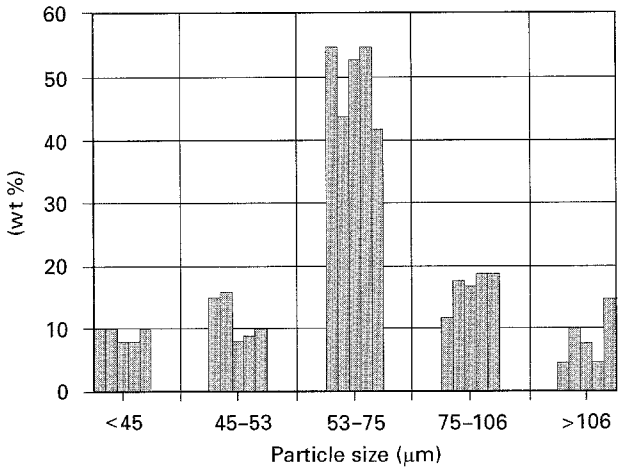

Figure 4 Sieve analysis of precipitator fly ash.

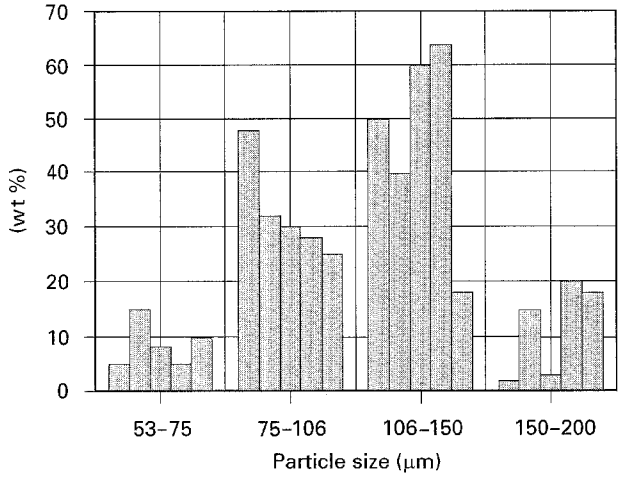

Figure 5 Sieve analysis of cenosphere fly ash.

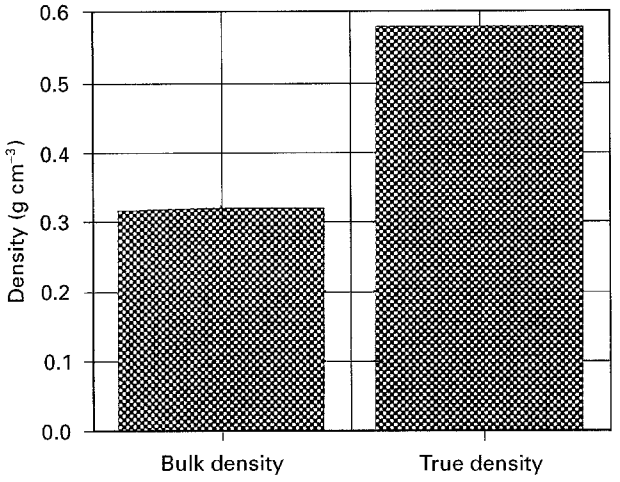

Figure 7 Density of as-received cenosphere fly ash.

(0.3–0.6 g cm^{-3}), and therefore may be used to produce ultralight metal matrix composites, which may find applications in automotive applications. For these ultralight applications, the hollow fly ash particles should be preserved in their hollow form during processing.

The apparent density of aluminium–fly ash (precipitator) powder mixture as a function of fly ash weight per cent was determined and the data indicate that the apparent density of aluminium–fly ash (precipitator) mixture is not significantly affected by additions of fly ash within the range investigated.

3.2. Compacting characteristics

The green density of aluminium–fly ash (precipitator) compacts as a function of compacting pressure is shown in Fig. 8. It is apparent from this figure that green density increases with increasing compacting pressure. The increase in green density of

TABLE I Chemical composition of fly ash particle (wt %)

Type of fly ash	SiO_2	Al_2O_3	Fe_2O_3	CaO	SO_3	MgO	K_2O	Na_2O	TiO_2
Precipitator	38.5	17.1	25.1	4.00	1.90	1.10	2.50	0.50	1.50
Cenosphere	60.8	25.9	4.50	0.72	0.26	1.58	3.58	0.80	1.00

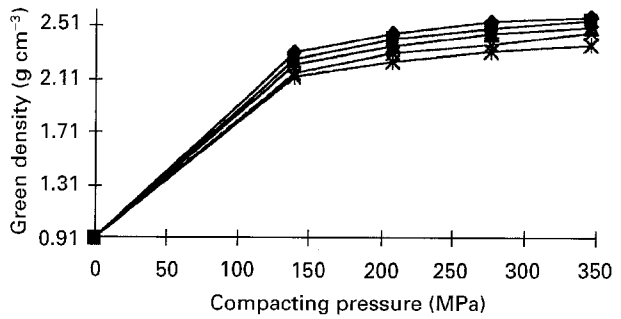

Figure 8 The green density of aluminium–precipitator fly ash powder compacts under various compacting pressure (time under pressure 1 min): (◆) Al, (■) Al–5 wt % fly ash, (▲) Al–10 wt % fly ash, (×) Al–35 wt % fly ash (*) Al–20 wt % fly ash.

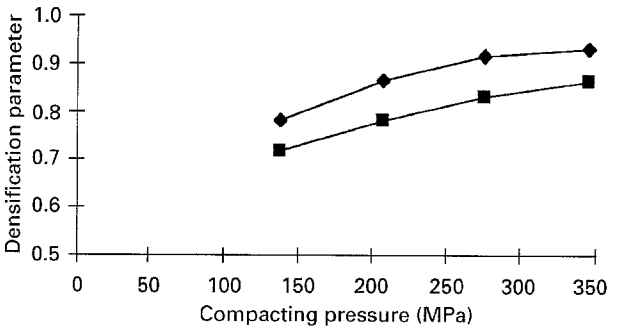

Figure 9 Effect of compacting pressure on the densification parameter for (◆) Al-5 wt % precipitator fly ash and (■) and Al–20 wt % precipitator fly ash.

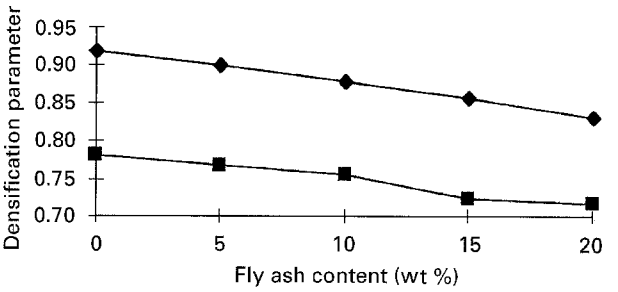

Figure 10 Effect of precipitator fly ash content on the densification parameter: compacting pressure (◆) 276 MPa, (■) 138 MPa.

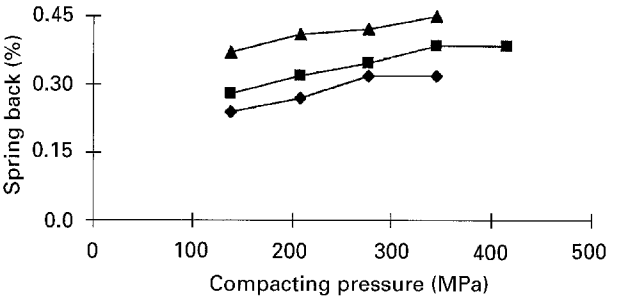

Figure 11 Effect of compacting pressure on the spring back of both aluminium–precipitator and aluminium–cenosphere compacts: (◆) Al, (■) Al-10 wt % precipitator, (▲) Al–10 wt % cenosphere.

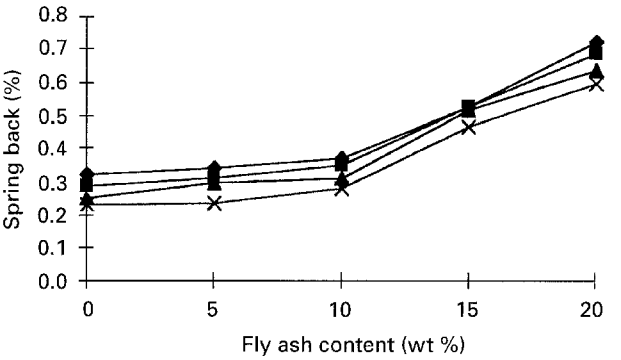

Figure 12 Effect of precipitator fly ash content on spring back. Compacting pressure: (◆) 345 MPa, (■) 276 MPa, (▲) 207 MPa, (×) 138 MPa.

aluminium–fly ash compacts with increase in pressure for a fixed fly ash (precipitator) content can be attributed to the reduction in porosity as a result of filling of empty spaces existing between particles by the solid powder during consolidation at different compacting pressures. The data also indicate that compact densities at all pressures progressively decrease with increasing fly ash amount because the true fly ash (precipitator) density is about 2.1 g cm^{-3} and the true aluminium density is 2.7 g cm^{-3}. As the fly ash particle volume increases, the compacts exhibit a reduction in green density for similar compacting conditions. This is attributed to the lower density of fly ash powder as compared to that of aluminium powder. Compacting time has no significant influence on the density of compacts.

The densification parameter as a function of compacting pressure and precipitator fly ash weight per cent is shown in Figs 9 and 10, respectively. It is clear from these figures that densification increases with increase in pressure and decreases with an increase of fly ash content.

The per cent spring back as a function of compacting pressure for aluminium and aluminium–fly ash compacts containing 10 wt % fly ash (both precipitator and cenosphere) is shown in Fig. 11. The increase in spring back with increasing pressure (Fig. 11) may be due to increasing plastic strain.

Fig. 12 shows the per cent spring back as a function of fly ash (precipitator) content. According to this figure, the spring back increases with an increase in fly ash content. Spring back is strongly influenced by particles with a high yield strength and a low elastic modulus, and it increases with the amount of plastic deformation. In this investigation, the relative increase in spring back, as fly ash is introduced in the compacts, can be attributed to its deformation mode. Under the compression forces, most fly ash particles are either fractured or deformed in the elastic regime. The contribution of fly ash particles to spring back may be due to their elastic recovery, after the compacting pressure is removed.

Comparing the effects of precipitator and cenosphere fly ash on spring back, it is clear from Fig. 11 that for the same weight per cent and compacting pressures, cenosphere fly ash results in higher spring back. This can be attributed to the lower density of cenospheres as compared to that of precipitator fly ash particles resulting in higher volume fraction for the same weight per cent. The difference in spring back for the two types of fly ash may also result from the difference in deformation and fracture mode of particles under load, as indicated in Fig. 13a and b. It is

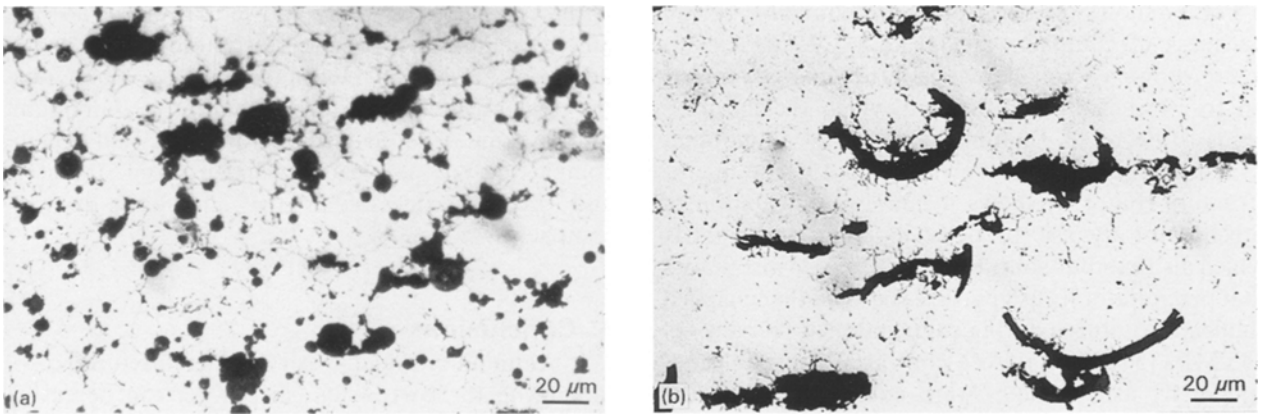

Figure 13 Photomicrographs of aluminium–fly ash compacts, at a compacting pressure of 345 MPa (50 000 p.s.i). (a) Al–10 wt % precipitator fly ash, (b) Al–5 wt % cenosphere fly ash.

clear from these figures that under similar compaction pressures, precipitator fly ash particles do not tend fracture, whereas cenosphere fly ash particles collapse and fracture, and the fragments of the walls of the cenospheres form a layered structure. The spherical fragments of fly ash spheres get dispersed in the matrix and the hollow spaces appear to get filled in by the matrix aluminium (Fig. 13b). Fig. 14 schematically shows that on processing, cenosphere fly ash collapses and fractures. Apparently much lower compacting pressures would be permissible if the fly ash cenospheres are to be retained in their assigned hollow sphere form.

The effect of compacting pressure on the green strength of aluminium–fly ash powder compacts containing different types of fly ash powder is shown in Fig. 15. This figure indicates that green strength increases with an increase in compacting pressure. This is attributed to increasing densification and particle-to-particle bonding, and possible interlocking of particles at increasing pressures. Fig. 15 indicates that the green strength of the aluminium–cenosphere compact was greater than that of aluminium–precipitator fly ash one. This can again be attributed to the difference in deformation modes of the two types of particles (Fig. 13a and b). The rupture of cenospheres and the dispersion of spherical fragments in a layered form in the aluminium matrix might provide better interlocking with aluminium particles, and a ribbon-type reinforcement from fragments, resulting in a higher strength in aluminium–cenosphere compacts as compared to aluminium–precipitator fly ash particle compacts. The effect of fly ash particle weight fraction on the green strength is shown in Fig. 16. This figure indicates a slight decrease in the strength of the compact with increasing amounts of fly ash particles especially above 10% fly ash. Above these levels, the fly ash particles in the compact may inhibit the mechanical interlocking and bonding between the metallic aluminium powders thereby decreasing the strength of the compacts (Fig. 16). The mechanical bonding between fly ash and aluminium particles can be low due to the smooth spherical surfaces of fly ash particles and the lack of plasticity of fly ash as compared to that of aluminium.

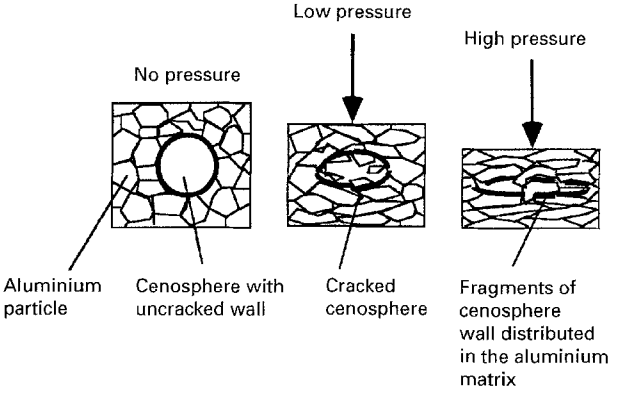

Figure 14 The sketch of the deformation process during compacting of aluminium–cenosphere particle mixture.

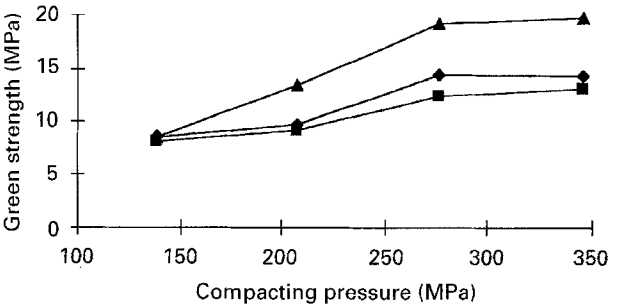

Figure 15 Effect of compacting pressure on the green strength for (◆) aluminium, (■) Al–10 wt % precipitator fly ash and (▲) Al–10 wt % cenosphere fly ash compacts.

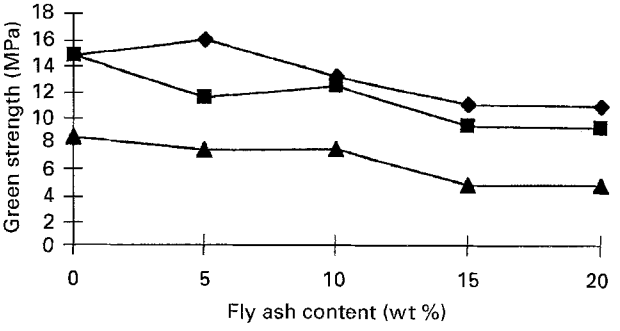

Figure 16 Effect of precipitator fly ash content on the green strength of aluminium-fly ash compacts under compacting pressures of (▲) 138, (■) 276 and (◆) 345 MPa, respectively.

Fig. 17 shows the effect of fly ash content on green hardness of compacts produced at 345 MPa. This figure shows a small change in hardness of compacts up to 10 wt % fly ash, beyond which the hardness tends to decrease. Photomicrographs of aluminium-fly ash compacts were shown in Fig. 13. The microstructure (Fig. 13a) shows a uniform distribution of precipitator fly ash particles in aluminium matrix which also exhibits some porosity. Fig. 13a also shows that precipitator fly ash particles have neither changed shape nor ruptured during compaction at pressures of 345 MPa (50 000 p.s.i). As a contrast, almost all cenosphere fly ash particles were collapsed during the compacting process at applied compacting pressure, as shown in Fig. 13b. Scanning electron micrographs of aluminium–10 wt % precipitator fly ash compacts are shown in Fig. 18. It can be seen from Fig. 18 that, at compacting pressures, the plastic deformation of aluminium particles is more and the extent of porosity in the compact considerably lower. However, no significant deformation of the precipitator fly ash particles can be seen in these micrographs. Apparently, the greater degree of plastic deformation of aluminium powders and reduced porosity obtained under high compacting pressure leads to higher green strengths and green hardnesses in the aluminium-fly ash compacts.

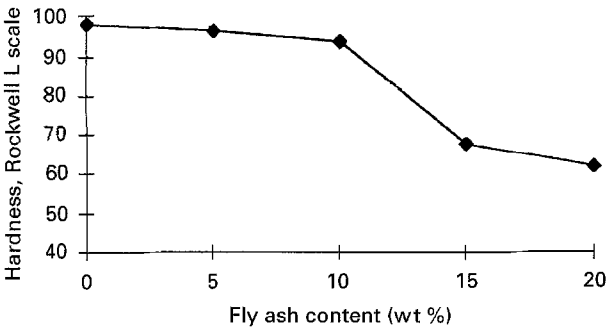

Figure 17 Effect of precipitator fly ash content on the green hardness of compacts, with a compacting pressure of 345 MPa, and a compacting time of 1 min (using Rochwell L scale).

4. Conclusions

1. Aluminium and fly ash powder mixtures containing up to 20 wt % fly ash powder can be easily compacted.
2. The green density of the compacts increases with an increase in the compacting pressure and decreases with increasing fly ash content.
3. The green strength of the aluminium–fly ash powder compacts increases with increasing compacting pressure and decreases with increasing fly ash content.
4. The morphology, of aluminium powders in compacts changed due to plastic deformation at compacting pressures in the range of 345 MPa.
5. Precipitator fly ash particles generally are neither changed in shape nor ruptured during compacting under pressure up to 345 MPa (50 000 p.s.i).
6. The cenosphere fly ash particles were observed to rupture under a compaction pressure of 345 MPa with the fragments of their walls distributed in the matrix in a layered structure, with the matrix filling the hollow spaces. This suggests that much lower compaction pressures will be permissible if the low-density hollow spheres are to be retained intact during powder processing.

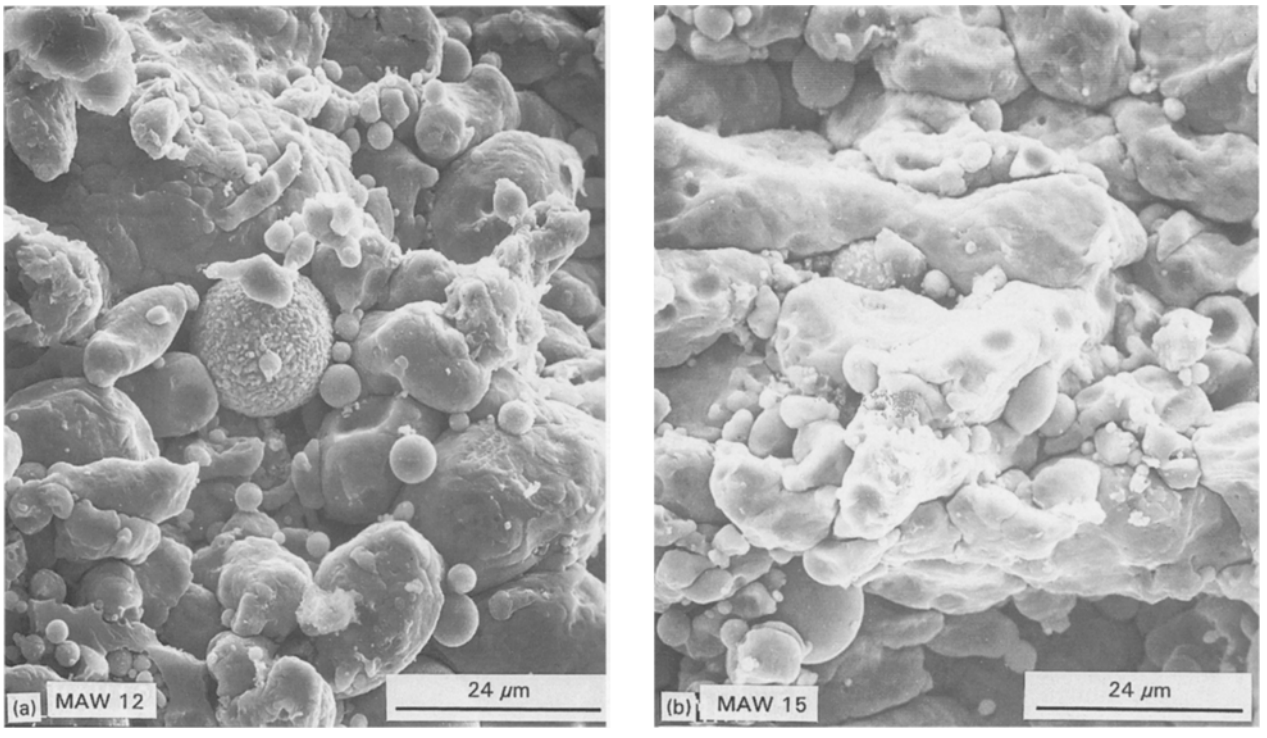

Figure 18 Scanning electron micrographs of Al–10 wt % precipitator fly ash compacts: (a) compacting pressure 138 MPa, (b) compacting pressure 345 MPa.

7. Spring back as well as green strength of compacts of aluminium–cenosphere fly ash was higher compared to that of aluminium–precipitator fly ash.

8. The hardness of the composite compacts containing 0–10 wt % fly ash did not change significantly up to 15 wt % fly ash; above 15 wt % fly ash levels, the hardness showed significant decreases.

References

1. P. K. ROHATGI, *J. Metals* November (1994) 55.
2. P. K. ROHATGI, B. N. KESHAVARAM, P. HUANG, R. GUO, D. M. GOLDEN, S. REINHARDT and D. ODOR, in "Proceedings of the Tenth International Ash Use Symposium", January 1993, edited by D. M. Golden, pp. 76–1.
3. G. F. BRENDEL, in "Proceedings of the 11th International Symposium on Use and Management of Coal Combustion By-Products (CCB's)", January 1995, edited by S. S. Tyson, pp. 66–1.
4. S. JALAI, *ibid.*, pp. 68–1.
5. P. K. ROHATGI, R. ASTHANA and S. DAS, *Int. Metals Revs.* (1986) 115.
6. D. NATH, RAM NARAYAN and P. K. ROHATGI, *J. Mater. Sci.* **16** (1981).
7. D. NATH, S. K. BISWAS and P. K. ROHATGI, *Wear* **60** (1980) 61.

Received 6 February
and accepted 24 April 1996